

Lepton flavor violation in predictive supersymmetric GUT models

Carl H. Albright^{1,2,*} and Mu-Chun Chen^{3,†}

¹*Department of Physics, Northern Illinois University, DeKalb, IL 60115*

²*Fermi National Accelerator Laboratory, Batavia, IL 60510*

³*Department of Physics & Astronomy,
University of California, Irvine, CA 92697*

(Dated: March 12, 2008)

Abstract

There have been many theoretical models constructed which aim to explain the neutrino masses and mixing patterns. While many of the models will be eliminated once more accurate determinations of the mixing parameters, especially $\sin^2 2\theta_{13}$, are obtained, charged lepton flavor violation experiments are able to differentiate even further among the models. In this paper, we investigate various rare lepton flavor violation processes, such as $\ell_i \rightarrow \ell_j + \gamma$ and $\mu - e$ conversion, in five predictive supersymmetric (SUSY) $SO(10)$ models and their allowed soft-SUSY breaking parameter space in the constrained minimal SUSY standard model. Utilizing the Wilkinson Microwave Anisotropy Probe dark matter constraints, we obtain lower bounds on the branching ratios of these rare processes and find that at least three of the five models we consider give rise to predictions for $\mu \rightarrow e + \gamma$ that will be tested by the MEG Collaboration at PSI. In addition, the next generation $\mu - e$ conversion experiment has sensitivity to the predictions of all five models, making it an even more robust way to test these models. While generic studies have emphasized the dependence of the branching ratios of these rare processes on the reactor neutrino angle, θ_{13} , and the mass of the heaviest right-handed neutrino, M_3 , we find very massive M_3 is more significant than large θ_{13} in leading to branching ratios near to the present upper limits.

PACS numbers: 14.60.Pq, 12.10.Dm, 12.15.Ff

*Electronic address: albright@fnal.gov

†Electronic address: muchunc@uci.edu

I. INTRODUCTION

The recent compilation of oscillation data from the atmospheric [1], reactor [2], and long baseline [3] neutrino experiments has provided solid evidence that neutrinos have small but non-zero masses. A global fit to current data gives the following 2σ limits for the mixing parameters [4],

$$\sin^2 \theta_{12} = (0.28 - 0.37), \quad \Delta m_{21}^2 = (7.3 - 8.1) \times 10^{-5} \text{ eV}^2 \quad (1)$$

$$\sin^2 \theta_{23} = 0.38 - 0.63, \quad \Delta m_{31}^2 = (2.1 - 2.7) \times 10^{-3} \text{ eV}^2 \quad (2)$$

$$\sin^2 \theta_{13} < 0.033 . \quad (3)$$

Since then, the measurements of neutrino oscillation parameters have entered a precision era. On the other hand, as no information exists for the value of θ_{13} , the Dirac or Majorana nature of the neutrinos, the Dirac and/or Majorana CP phases, and the neutrino mass hierarchy, there are discoveries that are still yet to come.

In the Standard Model (SM), due to the lack of right-handed neutrinos and the conservation of lepton numbers, neutrinos are massless. To generate non-zero neutrino masses thus calls for physics beyond the SM. There have been many theoretical ideas proposed with an attempt to accommodate the experimentally observed small neutrino masses and the larger mixing angles among them. In Ref. [5], we have surveyed 63 models in the literature that are still viable candidates and have reasonably well-defined predictions for θ_{13} . We found that the predictions for $\sin^2 2\theta_{13}$ of half of the models cover the range from 0.015 to the present upper bound of 0.13. Consequently, half of the models can be eliminated in the next generation of reactor experiments.

One of the implications of the observation of neutrino oscillation is the possibility of measurable branching ratio for charged lepton flavor-violating (LFV) decays. While not the case in the SM, predictions of the supersymmetric (SUSY) Grand Unified Theories (GUT) for these rare decays are much enhanced, as these processes are suppressed by the SUSY scale, rather than the Plank scale [6]. Furthermore, as different models obtain large neutrino mixing angles through different mechanisms, their predictions for the LFV charged lepton decays can be very distinct. Consequently, LFV charged lepton decays may provide a way to distinguish different SUSY GUT models.

Among the models aiming to explain the neutrino masses and mixing, a particularly promising class are those based on (SUSY) SO(10); for recent reviews of SO(10) models, see [7]. In this paper, we investigate the predictions for various LFV charged lepton decays as well as muon-electron conversion in five of the SUSY SO(10) models, assuming constrained minimal SUSY standard model (CMSSM) boundary conditions where only five soft-SUSY breaking parameters

are present. Furthermore, we impose the Wilkinson Microwave Anisotropy Probe (WMAP) dark matter constraints in the neutralino, stau and stop coannihilation regions. Specifically, we present the allowed values for these soft-SUSY parameters for various branching ratios of these rare LFV processes. In addition, the lower bounds on the predictions for these rare processes in the five different SUSY SO(10) models are given. We find that the predictions in these models are very distinct. We note the crucial role of the WMAP constraints in deducing the lower bounds on the predictions.

Many authors have previously studied the branching ratio predictions for charged LFV decays in the SUSY GUT framework. Rather than study specific models, they generally adopt a generic approach and assume a nearly diagonal Cabibbo-Kobayashi-Maskawa (CKM)-like or bimaximal Pontecorvo-Maki-Nakagawa-Sakata (PMNS)-like mixing matrix to diagonalize the Yukawa neutrino matrix [8]. Following the procedure of Casas and Ibarra [9] to invert the seesaw formula, they have carried out Monte Carlo studies by scanning the unknown right-handed neutrino mass spectrum and the angles and phases of the inversion matrix in order to present scatter plots of the rare branching ratios. A few exceptions to this procedure can be found in Ref. [10]. Here we are interested in specific models in order to determine the ability of the LFV experiments to differentiate among and rule out some models. The models chosen are highly predictive and illustrate a wide variety of textures for the charged lepton and neutrino mass matrices, and predictions for the right-handed neutrino mass spectrum and the reactor neutrino mixing angle, θ_{13} .

In Sec. II we describe the five representative SUSY SO(10) models that we have analyzed. In Sec. III we review LFV charged lepton decays in the SM and SUSY GUTs and present the predictions for the five SUSY SO(10) models considered. In Sec. IV their expectations for $\mu - e$ conversion are given. Sect. V concludes this paper.

II. PREDICTIVE SUPERSYMMETRIC GRAND UNIFIED MODELS CONSIDERED

We begin with a brief discussion of the general formalism on which the supersymmetric SO(10) grand unified models are based. For all five models to be illustrated, the seesaw mechanism [11] is of the conventional type I leading to normal hierarchies for the light Majorana neutrinos. The leptonic sector of the Yukawa superpotential at the GUT scale can then be written as

$$W_Y = N_i^c Y_{ij}^\nu L_j H_u + E_i^c Y_{ij}^e L_j H_d + N_i^c M_{Rij} N_j^c, \quad (4)$$

where L represents the left-handed lepton doublet, N^c the left-handed conjugate neutrino

singlet, and E^c the left-handed conjugate charged lepton of one of the three **16** dimensional representations of $SO(10)$. When the two Higgs doublets, H_u and H_d , acquire vacuum expectation values, the charged lepton and neutrino mass matrices are generated and can be written in 6×6 form

$$\begin{aligned}\mathcal{M}^e &= \begin{pmatrix} e_L^T & e_L^{cT} \end{pmatrix} \begin{pmatrix} 0 & M_E^T \\ M_E & 0 \end{pmatrix} \begin{pmatrix} e_L \\ e_L^c \end{pmatrix}, \\ \mathcal{M}^\nu &= \begin{pmatrix} \nu_L^T & N_L^{cT} \end{pmatrix} \begin{pmatrix} 0 & M_N^T \\ M_N & M_R \end{pmatrix} \begin{pmatrix} \nu_L \\ N_L^c \end{pmatrix}.\end{aligned}\tag{5}$$

With the entries in M_R much larger than those in M_N , the light Majorana neutrino mass matrix is given by the well-known type I seesaw formula [11],

$$M_\nu = -M_N^T M_R^{-1} M_N.\tag{6}$$

Note that the above Dirac 3×3 mass matrix entries, M_E and M_N , are written in right - left order and appear in the $SO(10)$ flavor basis. As such, the matrices can be diagonalized by the unitary transformations

$$\begin{aligned}U_{ER}^\dagger M_E U_{EL} &= \text{diag}(m_e, m_\mu, m_\tau), \\ U_{MR}^\dagger M_R U_{MR}^* &= \text{diag}(M_1, M_2, M_3), \\ U_{\nu L}^T M_\nu U_{\nu L} &= \text{diag}(m_1, m_2, m_3),\end{aligned}\tag{7}$$

by forming the Hermitian products, calculating the left and right unitary transformations of column eigenvectors, and phase rotating the complex symmetric M_R and M_ν matrices, so their mass eigenvalues are real. The PMNS neutrino mixing matrix [12] is then given by $V_{PMNS} = U_{EL}^\dagger U_{\nu L}$.

On the other hand for later use, it is convenient to transform to the bases where M_E and M_R are diagonal and denoted by primed quantities. In this case

$$\begin{aligned}M'_\nu &= -M_N'^T M_R'^{-1} M'_N, \\ U_{\nu L}'^T M'_\nu U_{\nu L}' &= \text{diag}(m_1, m_2, m_3),\end{aligned}\tag{8}$$

where now $V_{PMNS} = U_{\nu L}'$, since U_{EL}' is just the identity matrix. A comparison of the seesaw diagonalization matrices then reveals that the transformed Dirac neutrino matrix M'_N in the new basis is given by

$$M'_N = U_{MR}^\dagger M_N U_{EL},\tag{9}$$

in terms of the original matrix in the flavor bases.

With either basis, the left-handed neutrino PMNS mixing matrix can be written as $V_{PMNS} = U_{PMNS}\Phi$, where by convention [13]

$$U_{PMNS} = \begin{pmatrix} c_{12}c_{13} & s_{12}c_{13} & s_{13}e^{-i\delta} \\ -s_{12}c_{23} - c_{12}s_{23}s_{13}e^{i\delta} & c_{12}c_{23} - s_{12}s_{23}s_{13}e^{i\delta} & s_{23}c_{13} \\ s_{23}s_{12} - c_{12}c_{23}s_{13}e^{i\delta} & -c_{12}s_{23} - s_{12}c_{23}s_{13}e^{i\delta} & c_{23}c_{13} \end{pmatrix} \quad (10)$$

in terms of the three mixing angles, θ_{12} , θ_{23} and θ_{13} ; and the Dirac CP phase, δ , in analogy with the quark mixing matrix. The Majorana phase matrix,

$$\Phi = \text{diag}(e^{i\chi_1}, e^{i\chi_2}, 1), \quad (11)$$

written in terms of the two Majorana phases, χ_1 and χ_2 , is required since an arbitrary phase transformation is not possible when one demands real diagonal neutrino mass entries in the transformation of M_ν in Eq. (7) or M'_ν in Eq. (8).

With this background in mind, we now turn to a brief discussion of the five $SO(10)$ models we have considered for our lepton flavor violation study. The $SO(10)$ grand unification symmetry is an economical and attractive one [7], for all sixteen left-handed quark and lepton fields and their left-handed conjugates fit neatly into one **16** representation per family. Many models exist in the literature which differ from one another by their Higgs representation assignments and type of flavor symmetry imposed, if any. To appreciate this, it is of interest to note the following decompositions of the direct product of representations:

$$\begin{aligned} \mathbf{16} \otimes \mathbf{16} &= \mathbf{10}_s \oplus \mathbf{120}_a \oplus \mathbf{126}_s, \\ \mathbf{16} \otimes \overline{\mathbf{16}} &= \mathbf{1} \oplus \mathbf{45} \oplus \mathbf{210}, \end{aligned} \quad (12)$$

where in the first product the **10** and **126** matrices are symmetric, while the **120** is antisymmetric under the interchange of family indices.

Given this group structure for $SO(10)$, there are two general classes of models which have been extensively studied. Those with Higgs in the **10**, **126**, $\overline{\mathbf{126}}$, and possibly the **120** and/or **210**, dimensional representations are often referred to as the minimal Higgs models [14] and lead to symmetric or antisymmetric matrix elements, or a superposition of the two. The advantage is that the couplings are renormalizable and preserve R-parity, but the latter representations are of rather high rank and disfavored in the string theory framework. The other class typically involves the lower rank Higgs representations such as **10**, **16**, $\overline{\mathbf{16}}$, **45**, with some non-renormalizable effective operators formed from them, [15] but R-parity is not conserved. They can lead to lopsided mass matrices for the charged lepton and down quark mass matrices, due to the $SU(5)$ structure present

in the **16**'s. As such, one may anticipate that they will predict a higher level of lepton flavor violation than the first class. The $SU(2)_L$ triplet components in the Higgs representations in all five models considered have no electroweak VEV and hence lead to the conventional type I seesaw mechanism with the prediction of normal hierarchy for the light left-handed neutrino spectrum [16]. We elaborate on each model in turn but give only the neutrino and charged lepton mass matrices. All successfully predict the observed quark structure and CKM mixings.

A. Albright - Barr $SO(10)$ Model

This model, based on $SO(10)$ with a $U(1) \times Z_2 \times Z_2$ flavor symmetry [17], is of the lopsided variety and has matrices of the following textures:

$$M_N = \begin{pmatrix} \eta & \delta_N & \delta'_N \\ \delta_N & 0 & -\epsilon \\ \delta'_N & \epsilon & 1 \end{pmatrix} m_U, \quad M_E = \begin{pmatrix} 0 & \delta & \delta' \\ \delta & 0 & -\epsilon \\ \delta' & \sigma + \epsilon & 1 \end{pmatrix} m_D, \quad (13)$$

where the parameters have the values $\eta = 1.1 \times 10^{-5}$, $\epsilon = 0.147$, $\sigma = 1.83$, $\delta = 0.00946$, $\delta' = 0.00827e^{i119.4^\circ}$, $\delta_N = -1.0 \times 10^{-5}$, $\delta'_N = -1.5 \times 10^{-5}$, $m_U = 113$ GeV, $m_D = 1$ GeV. The right-handed Majorana mass matrix is given by

$$M_R = \begin{pmatrix} c^2\eta^2 & -b\epsilon\eta & a\eta \\ -b\epsilon\eta & \epsilon^2 & -\epsilon \\ a\eta & -\epsilon & 1 \end{pmatrix} \Lambda_R, \quad (14)$$

where $a = c = 0.5828i$, $b = 1.7670i$, $\Lambda_R = 2.35 \times 10^{14}$ GeV. One finds

$$\begin{aligned} M_1 &\simeq M_2 \simeq 4.45 \times 10^8 \text{ GeV}, & M_3 &= 2.4 \times 10^{14} \text{ GeV}, \\ m_1 &= 3.11 \text{ meV}, & m_2 &= 9.48 \text{ meV}, & m_3 &= 49.13 \text{ meV}, \\ \Delta m_{21}^2 &= 8.0 \times 10^{-5} \text{ eV}^2, & \Delta m_{32}^2 &= 2.3 \times 10^{-3} \text{ eV}^2, \\ \sin^2 2\theta_{23} &= 0.99, & \sin^2 \theta_{12} &= 0.28, & \sin^2 \theta_{13} &= 0.0020. \end{aligned} \quad (15)$$

A value of $\tan \beta = 5$ assures that $\sigma \gg \epsilon$ and that the corresponding lopsided nature of the 23 element of the down quark mass matrix gives a good fit to the results for the quark sector. The δ_N , δ'_N elements of the Dirac neutrino matrix were added [18] to the original model to give a better fit to baryogenesis arising from resonant leptogenesis involving the two lighter right-handed neutrinos [19]. Evolution downward from the GUT scale to M_Z has little effect on the mixing angles due to the small $\tan \beta$, the opposite CP-parity of the lighter two right-handed Majorana neutrinos, and their large hierarchy with the heaviest one; but serves to lower the values of the m_i 's and Δm_{32}^2 and Δm_{21}^2 relative to their GUT scale values.

B. Chen - Mahanthappa $SO(10)$ Model

This model, based on $SO(10)$ with a $SU(2) \times Z_2 \times Z_2 \times Z_2$ flavor symmetry [20], is of the minimal Higgs variety leading to symmetric entries in the mass matrices:

$$M_N = \begin{pmatrix} 0 & 0 & a \\ 0 & be^{i\theta} & c \\ a & c & 1 \end{pmatrix} vd \sin \beta, \quad M_E = \begin{pmatrix} 0 & ee^{-i\phi} & 0 \\ ee^{i\phi} & -3f & 0 \\ 0 & 0 & 1 \end{pmatrix} vh \cos \beta, \quad (16)$$

where $v = 174$ GeV and the parameters have the values $a = 0.00250$, $b = 0.00326$, $c = 0.0346$, $d = 0.650$, $e = 0.004036$, $f = 0.0195$, $h = 0.06878$, $\theta = 0.74$, $\phi = -1.52$. The solar and atmospheric neutrino mass squared differences, $\Delta m_{\text{sol}}^2 = 8.14 \times 10^{-5} \text{ eV}^2$ and $\Delta m_{32}^2 = 2.3 \times 10^{-3} \text{ eV}^2$ were used as input to determine the $t = 0.344$ and $M_3 = 6.97 \times 10^{12}$ parameters in the effective light left-handed Majorana neutrino mass matrix

$$M_{\nu_L} = \begin{pmatrix} 0 & 0 & t \\ 0 & 1 & 1+t^n \\ t & 1+t^n & 1 \end{pmatrix} \frac{(vd \sin \beta)^2}{M_R}, \quad (17)$$

One then finds

$$\begin{aligned} M_1 &= 1.09 \times 10^7 \text{ GeV}, \quad M_2 = 4.53 \times 10^9 \text{ GeV}, \quad M_3 = 6.97 \times 10^{12} \text{ GeV}, \\ m_1 &= 2.62 \text{ meV}, \quad m_2 = 9.39 \text{ meV}, \quad m_3 = 49.2 \text{ meV}. \\ \sin^2 2\theta_{23} &= 1.00, \quad \sin^2 \theta_{12} = 0.27, \quad \sin^2 \theta_{13} = 0.013. \end{aligned} \quad (18)$$

For this model, a value of $\tan \beta = 10$ is used. The effect of evolution from the GUT scale to M_Z is to raise $\sin^2 \theta_{12}$ and to lower $\sin^2 \theta_{13}$.

C. Cai - Yu $SO(10)$ Model

This model is based on $SO(10)$ with an S_4 flavor symmetry [21]. The Higgs fields appear in six **10**'s, three $\overline{\mathbf{126}}$'s, three **126**, and one **210** representations of $SO(10)$, distinguished by their S_4 flavor assignments. Of the 14 pairs of Higgs doublets at the GUT scale, all but one pair are assumed to get superheavy. The charged lepton mass matrix is chosen to be diagonal, while the right-handed Majorana neutrino mass matrix is proportional to the identity matrix, so all three heavy neutrinos

are degenerate. The Dirac neutrino and charged lepton mass matrices are symmetric and given by

$$\begin{aligned}
M_N &= \begin{pmatrix} a_0 - 2a_2 - 3(d_0 - 2d_2) & a_5 & a_4 \\ a_5 & a_0 + a_1 + a_2 - 3(d_0 + d_1 + d_2) & a_3 \\ a_4 & a_3 & a_0 - a_1 + a_2 - 3(d_0 - d_1 + d_2) \end{pmatrix}, \\
M_E &= \begin{pmatrix} b_0 - 2b_2 - 3(e_0 - 2e_2) & 0 & 0 \\ 0 & b_0 + b_1 + b_2 - 3(e_0 + e_1 + e_2) & 0 \\ 0 & 0 & b_0 - b_1 + b_2 - 3(e_0 - e_1 + e_2) \end{pmatrix},
\end{aligned} \tag{19}$$

where the parameters have the values $a_0 = 18.935 + 0.000271681i$, $a_1 = -30.7989 + 0.0019887i$, $a_2 = 10.0361 + 0.00171701i$, $a_3 = -2.99072 - 0.054757i$, $a_4 = 0.554859 - 0.234705i$, $a_5 = -0.066748 + 0.008155i$, $b_0 = 0.387756$, $b_1 = -0.539649$, $b_2 = 0.19327$, $d_0 = 8.60218$, $d_1 = -10.1912$, $d_2 = 3.72519$, $e_0 = -0.0227734$, $e_1 = 0.0228717$, $e_2 = -0.0115298$, all in GeV. The common mass of the degenerate right-handed neutrinos is determined to be $M_R = 2.4 \times 10^{12}$ GeV, so as to fit $\Delta m_{31}^2 = 2.6 \times 10^{-3}$ eV² with the aid of the seesaw formula. The authors find

$$\begin{aligned}
m_1 &= 7.7 \text{ meV}, \quad m_2 = 11.8 \text{ meV}, \quad m_3 = 50.7 \text{ meV}, \\
\sin^2 2\theta_{23} &= 1.00, \quad \sin^2 \theta_{12} = 0.29, \quad \sin^2 \theta_{13} = 0.0029.
\end{aligned} \tag{20}$$

A value of $\tan \beta = 10$ is used to evolve the quark and charged lepton masses, though the neutrino masses and mixings have not been evolved downward to the electroweak scale.

D. Dermisek - Raby $SO(10)$ Model

This model is based on $SO(10)$ with a D_3 family symmetry [22]. The charged lepton and down quark mass matrices have lopsided textures, but they are not so extreme as in the case of the Albright - Barr model:

$$M_N = \begin{pmatrix} 0 & \epsilon' \omega & -3\epsilon \xi \sigma \\ -\epsilon' \omega & 3\tilde{\epsilon} \omega & -3\epsilon \sigma \\ 1.5\epsilon \xi \omega & 1.5\epsilon \omega & 1 \end{pmatrix} v \lambda \sin \beta, \quad M_E = \begin{pmatrix} 0 & \epsilon' & -3\epsilon \xi \sigma \\ -\epsilon' & 3\tilde{\epsilon} & -3\epsilon \sigma \\ 3\epsilon \xi & 3\epsilon & 1 \end{pmatrix} v \lambda \cos \beta, \tag{21}$$

where $v = 174$ GeV and the parameters have the values $\lambda = 0.64$, $\epsilon = 0.046$, $\sigma = 0.83e^{0.618i}$, $\tilde{\epsilon} = 0.011e^{0.411i}$, $\rho = -0.053e^{0.767i}$, $\epsilon' = -0.0036$, $\xi = 0.12e^{3.673i}$, $\omega = 2\sigma/(2\sigma - 1)$. The right-handed Majorana mass matrix is diagonal with mass eigenvalues $M_1 = 1.1 \times 10^{10}$, $M_2 = -9.3 \times 10^{11}$, $M_3 = 5.8 \times 10^{13}$ GeV. These parameters were chosen by making use of the central experimental

values for $\Delta m_{21}^2 = 7.9 \times 10^{-5} \text{ eV}^2$, $\Delta m_{31}^2 = 2.3 \times 10^{-3} \text{ eV}^2$, $\sin^2 \theta_{12} = 0.295$ and $\sin^2 \theta_{23} = 0.51$ at the time of writing. The authors find

$$\begin{aligned} m_1 &= 3.7 \text{ meV}, \quad m_2 = 9.6 \text{ meV}, \quad m_3 = 49.2 \text{ meV}, \\ \sin^2 \theta_{13} &= 0.0024. \end{aligned} \tag{22}$$

The evolution has been carried out with $\tan \beta = 49.98$ and $A_0 = -6888.3 \text{ GeV}$ down to M_Z and then down to the 1 GeV scale for the light neutrino masses.

E. Grimus - Kuhbock $SO(10)$ Model

This model is based on $SO(10)$ with an Z_2 flavor symmetry [23]. The Higgs fields appear in one each of the **10**, **120**, and $\overline{\mathbf{126}}$ dimensional representations of $SO(10)$. The fermion mass matrices are generated by renormalizable Yukawa couplings of these Higgs fields to the three families placed in **16**'s. The Dirac neutrino and charged lepton mass matrices are written as linear combinations of the Yukawa couplings of the **10**, **120**, and $\overline{\mathbf{126}}$ Higgs representations, respectively, while the right-handed Majorana matrix is proportional only to the latter:

$$\begin{aligned} M_N &= r_H H' + r_D e^{i\psi_D} G' - 3r_F e^{i\zeta_u} F', \\ M_E &= H' + r_L e^{i\psi_L} G' - 3e^{i\zeta_d} F', \\ M_R &= rR^{-1}F', \end{aligned} \tag{23}$$

where the individual Higgs contributions to the mass matrices are given by

$$\begin{aligned} H' &= \begin{pmatrix} 0.716986 & 0 & 0 \\ 0 & -40.6278 & 0 \\ 0 & 0 & 1114.41 \end{pmatrix} \times 10^{-3}, \\ G' &= \begin{pmatrix} 0 & -7.56737 & 0 \\ 7.56737 & 0 & -36.8224 \\ 0 & 36.8224 & 0 \end{pmatrix} \times 10^{-3}, \\ F' &= \begin{pmatrix} -0.0966851 & 0 & 4.25282 \\ 0 & 12.3136 & 0 \\ 4.25282 & 0 & -61.6491 \end{pmatrix} \times 10^{-3}, \end{aligned} \tag{24}$$

in the right-left order we have adopted. The coefficient parameters are taken to be $r_H = 91.0759$, $r_F = 297.758$, $r_u = 7.14572$, $r_L = 1.33897$, $r_D = 3008.88$, $r_R = 2.90553 \times 10^{-17}$, $\zeta_d = 19.66974^\circ$, $\zeta_u = -2.96594^\circ$, $\psi_L = 6.24258^\circ$, $\psi_D = 179.85271^\circ$. A value of $\tan \beta = 10$ is used to

evolve the quark and charged lepton masses downward to the electroweak scale. One finds then that

$$\begin{aligned} m_1 &= 1.6 \text{ meV}, & m_2 &= 9.2 \text{ meV}, & m_3 &= 50.0 \text{ meV}, \\ \sin^2 2\theta_{23} &= 1.00, & \sin^2 \theta_{12} &= 0.31, & \sin^2 \theta_{13} &= 0.00059. \end{aligned} \quad (25)$$

Although the results are impressive, the authors do note that 21 parameters have been introduced in order to obtain the results. Hence the model should be viewed as an existence proof that the lepton masses and mixings as well as the quark masses and mixings can be described in the framework of renormalizable couplings with only the three Higgs representations contributing to the Yukawa couplings.

We close this section by summarizing the features of these models in Table I. Three of the models have similar predictions for $\sin^2 \theta_{13} \sim 0.0025$, near the expected reach of the Double CHOOZ and Daya Bay reactor experiments [24]. One of the models predicts a value near the present upper

TABLE I: Higgs representations, flavor symmetries, and other noteworthy features of the five $SO(10)$ SUSY GUT models considered in this work.

Models	Higgs Content	Flavor Symmetry	M_R (GeV)	$\tan \beta$	$\sin^2 \theta_{13}$	Interesting Features
AB	10, 16, $\overline{16}$, 45	$U(1) \times Z_2 \times Z_2$	2.4×10^{14} 4.5×10^8 4.5×10^8	5	0.0020 (2.6°)	Large M_R hierarchy with lightest two nearly degenerate leads to resonant leptogenesis.
CM	10, $\overline{126}$	$SU(2) \times (Z_2)^3$	7.0×10^{12} 4.5×10^9 1.1×10^7	10	0.013 (6.5°)	Large M_R hierarchy with heaviest more than 3 orders of magnitude below GUT scale; large $\sin^2 \theta_{13}$.
CY	10, $\overline{126}$	S_4	2.4×10^{12} 2.4×10^{12} 2.4×10^{12}	10	0.0029 (3.1°)	Degenerate M_R spectrum 4 orders of magnitude below GUT scale.
DR	10, 45	D_3	5.8×10^{13} 9.3×10^{11} 1.1×10^{10}	50	0.0024 (2.8°)	Mild M_R hierarchy almost 3 orders of magnitude below GUT scale.
GK	10, 120, $\overline{126}$	Z_2	2.1×10^{15} 4.2×10^{14} 6.7×10^{12}	10	0.00059 (1.4°)	Mild M_R hierarchy just 1 order of magnitude below GUT scale; rather small $\sin^2 \theta_{13}$.

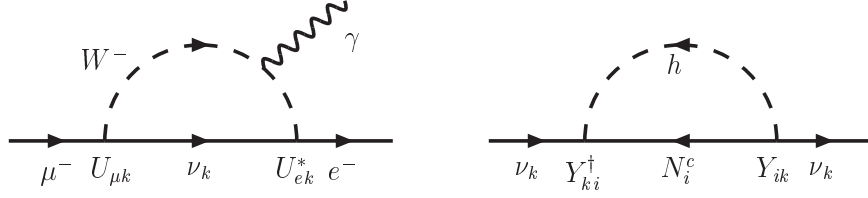


FIG. 1: Example of a Feynman diagram for $\mu \rightarrow e\gamma$ with a neutrino mass insertion in the SM.

limit placed by the CHOOZ experiment [25], while the fifth model predicts a value of 3×10^{-4} which is essentially beyond reach until a Neutrino Factory becomes a reality. We shall see what potential success charged lepton flavor violation experiments will have in further distinguishing the viable models.

III. LEPTON FLAVOR VIOLATION IN RADIATIVE DECAYS

We now turn to the subject of charged lepton flavor violation that can occur in the radiative decays, $\mu \rightarrow e + \gamma$, $\tau \rightarrow \mu + \gamma$, and $\tau \rightarrow e + \gamma$. In the SM with the addition of three massive right-handed neutrinos, we observe that the individual lepton numbers, L_e , L_μ and L_τ , are not individually conserved. In radiative lepton decays, the flavor violation arises in one loop, where the neutrino insertion involves lepton flavor-changing Yukawa couplings of the left-handed and right-handed neutrinos; cf. Fig. 1. The branching ratio BR21 defined by the ratio of the rate for the $\mu \rightarrow e\gamma$ mode relative to the purely leptonic mode, $\mu \rightarrow \nu_\mu e \bar{\nu}_e$, is given by [26]

$$\begin{aligned} BR21 &= \frac{3\alpha}{32\pi} \left| \sum_k U_{\mu k}^* \frac{m_k^2}{M_W^2} U_{ke} \right|^2 \\ &\simeq \frac{3\alpha}{128\pi} \left(\frac{\Delta m_{21}^2}{M_W^2} \right)^2 \sin^2 2\theta_{12} \sim 10^{-54}, \end{aligned} \quad (26)$$

where the U 's are elements of the PMNS mixing matrix. Hence in the SM, the expected branching ratio is immeasurably small, and the MEG experiment [27] looking for $\mu \rightarrow e\gamma$ would be expected to give a null result. The present upper limit of 1.2×10^{-11} was obtained by the MEGA collaboration [28].

In SUSY GUT models on the other hand, the leading log approximations involve slepton-neutralino and sneutrino-chargino loops which contribute to the radiative lepton decays [6]; cf. Fig. 2. With more comparable heavy masses of the SUSY particles in the loops and lack of a Glashow-Iliopoulos-Maiani (GIM) mechanism, such a great suppression of the branching ratio does not occur. We shall work in the CMSSM [29], where the soft-breaking scalar and gaugino masses and trilinear scalar couplings are assumed to be universal at the GUT scale. The lepton

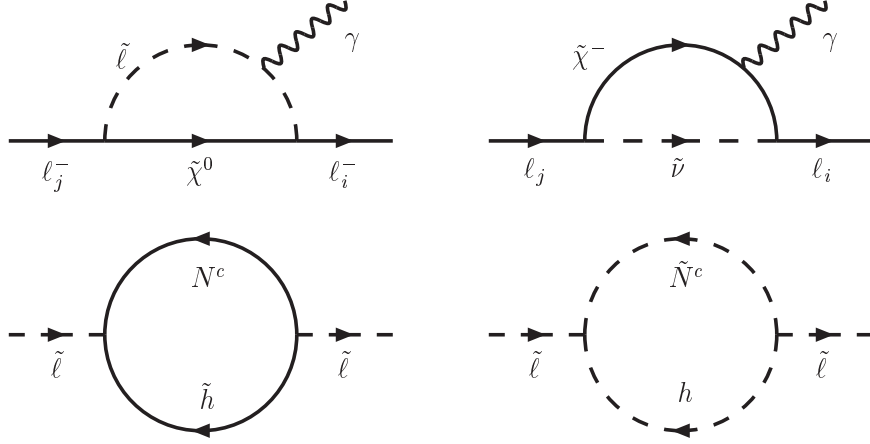


FIG. 2: Examples of Feynman diagrams for slepton - neutralino and sneutrino - chargino contributions to $\mu \rightarrow e\gamma$ in SUSY models with slepton mass insertions.

flavor violation then arises from evolution of the Yukawa couplings and soft-breaking parameters from the GUT scale down to the electroweak scale [30].

Feynman diagrams for the LFV radiative decays in leading log approximation involve both neutralino - slepton ($\tilde{\chi}^0 - \tilde{\ell}$) loops and chargino - sneutrino ($\tilde{\chi}^\pm - \tilde{\nu}$) loops with the emitted photon attached to the internal charged slepton or chargino, respectively. Through evolution from the GUT scale, the LFV neutrino Yukawa couplings are induced primarily in the mass squared submatrix for the $SU(2)_L$ doublet sleptons, $m_L^2(LL)$. We do not repeat the details here for this complicated calculation but rather refer the reader to the pioneering paper of Hisano, Moroi, Tobe, and Yamaguchi [30]. We simply note that the radiative decay rate is given by

$$\Gamma(\ell_j^- \rightarrow \ell_i^- \gamma) = \frac{e^2}{16\pi} m_{l_j}^5 \left(|A_L^{(n)} + A_L^{(c)}|^2 + |A_R^{(n)} + A_R^{(c)}|^2 \right), \quad (27)$$

where (n) and (c) refer to the neutralino and chargino loop contributions to the transition form factors A_L and A_R connecting leptons of opposite chirality. The branching ratio for the flavor-violating decay mode relative to the flavor-conserving purely lepton mode is then

$$BR(\ell_j^- \rightarrow \ell_i^- \gamma) = \frac{48\pi^3 \alpha}{G_F^2} (|A_L|^2 + |A_R|^2). \quad (28)$$

In the leading log approximation with the largest contribution coming from the left-handed slepton mass matrix, the branching ratio is given by

$$BRji = \frac{\alpha^3}{G_F^2 m_s^8} |(m_{LL}^2)_{ji}|^2 \tan^2 \beta, \quad (29)$$

where

$$(m_{LL}^2)_{ji} = -\frac{1}{8\pi^2} m_0^2 (3 + A_0^2/m_0^2) Y_{jk}^\dagger \log \left(\frac{M_G}{M_k} \right) Y_{ki}. \quad (30)$$

with the Yukawa couplings specified in the lepton flavor basis and the right-handed Majorana matrix diagonal, so M_k is just the k th heavy right-handed neutrino mass, while M_G is the GUT scale typically equal to 2×10^{16} GeV and m_s is some typical SUSY scalar mass. Petcov and collaborators [31] have shown that the full evolution effects as first calculated in [30] can be extremely well approximated by Eq. (29), if one sets

$$m_s^8 \simeq 0.5 m_0^2 M_{1/2}^2 (m_0^2 + 0.6 M_{1/2}^2)^2. \quad (31)$$

While the branching ratio for $\mu \rightarrow e + \gamma$ is well approximated by the above equations, the branching ratios for $\tau \rightarrow \mu + \gamma$ and $\tau \rightarrow e + \gamma$ must be scaled by the branching ratios for the flavor-conserving leptonic modes relative to their total decay rates.

We see that the MEG experiment [27] has no chance of observing a positive signal in the SM for the $\mu \rightarrow e\gamma$ decay channel; however, the situation will be totally different for the SUSY GUT models we have chosen to consider. In the CMSSM with universal soft-breaking parameters m_0 , $M_{1/2}$ and A_0 , for a given $\tan\beta$ and $\text{sgn}(\mu)$, we consider the following correlations between the branching ratio and the soft-SUSY breaking parameters:

- (a) the branching ratio *vs.* $M_{1/2}$ for fixed $A_0 = 0$, for example, with different choices of m_0 ;
- (b) the allowed parameter space for A_0/m_0 *vs.* $M_{1/2}$, for specific branching ratio ranges;
- (c) the branching ratio for $\tau \rightarrow \mu\gamma$ *vs.* that for $\mu \rightarrow e\gamma$, on a log-log plot, which are related by

$$\begin{aligned} \log \text{BR}(\tau \rightarrow \mu\gamma) &= \log \text{BR}(\mu \rightarrow e\gamma) + \log(\text{BR}32/\text{BR}21) + \log \text{BR}(\tau \rightarrow \nu_\tau \mu \bar{\nu}_\mu) \\ &= \log \text{BR}(\mu \rightarrow e\gamma) + \log \left| \frac{(Y_\nu^\dagger L Y_\nu)_{32}}{(Y_\nu^\dagger L Y_\nu)_{21}} \right|^2 - 0.757, \end{aligned} \quad (32)$$

where $L \equiv \log(M_G^2/M_R^2)$, and again the Yukawa matrices are converted to the lepton flavor basis with M_R diagonal. Due to the factorization of the soft-breaking parameters and the GUT model parameters in the approximate Eq. (29), the slope is unity, and the intercept is just the sum of the last two terms after correcting for the $\tau \rightarrow \nu_\tau \mu \bar{\nu}_\mu$ branching ratio. The length of the straight line segment depends on the range of the soft-breaking parameters chosen. A similar plot can be made for the branching ratio for $\tau \rightarrow e\gamma$ *vs.* that for $\mu \rightarrow e\gamma$.

For all three types of plots we have imposed the following soft parameter constraints [13]:

$$\begin{aligned}
\text{For } \tan \beta = 5, 10 : \quad m_0 : \quad & 50 \rightarrow 400 \text{ GeV} \\
& M_{1/2} : \quad 200 \rightarrow 1000 \text{ GeV} \\
& A_0 : -4000 \rightarrow 4000 \text{ GeV} \\
\text{For } \tan \beta = 50 : \quad m_0 : \quad & 500 \rightarrow 4000 \text{ GeV} \\
& M_{1/2} : \quad 200 \rightarrow 1500 \text{ GeV} \\
& A_0 : \quad -50 \rightarrow 50 \text{ TeV}
\end{aligned} \tag{33}$$

In addition it is desirable to impose WMAP dark matter constraints in the neutralino, stau or stop coannihilation regions [33], where the lightest neutralino is the LSP. These more restrictive constraints are well described by the quadratic polynomial for the soft scalar mass in terms of the soft gaugino mass [34]:

$$\begin{aligned}
m_0 &= c_0 + c_1 M_{1/2} + c_2 M_{1/2}^2, \\
c_i &= c_i(A_0, \tan \beta, \text{sgn}(\mu)).
\end{aligned} \tag{34}$$

where m_0 is bounded since $M_{1/2}$ is bounded. If $M_{1/2}$ is too small, the present experimental bound on the Higgs mass [13] of $m_h \gtrsim 114.4$ GeV may be violated or the neutralino relic density in the early universe will be too small, while if $M_{1/2}$ is too large the neutralino relic density will be too large. We shall impose both limits on the DM constraint conditions for various values of A_0 and find that both lower and upper limits are placed on the branching ratios for each model.

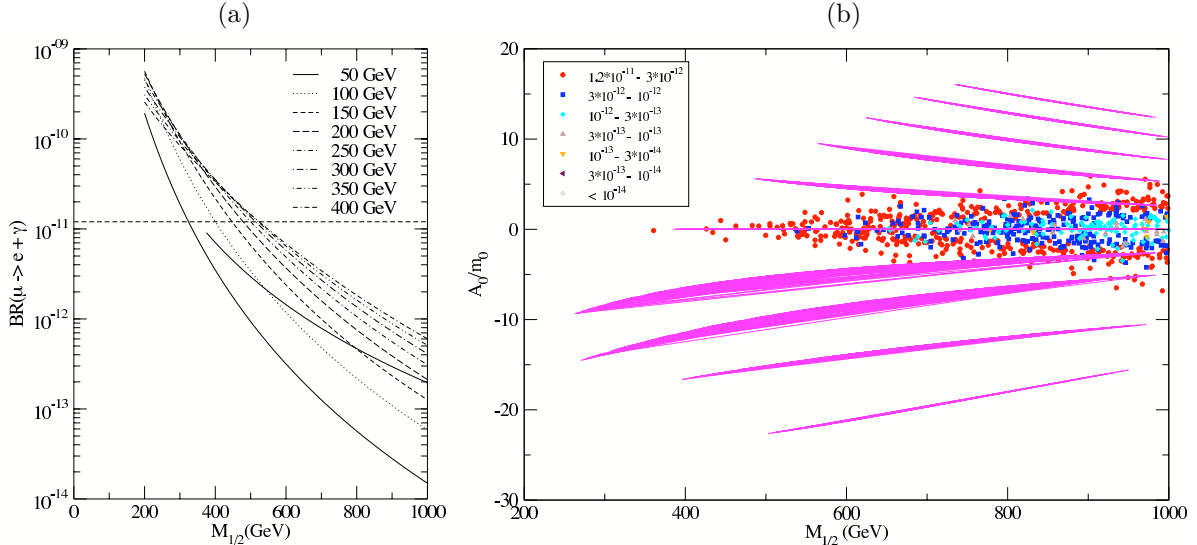


FIG. 3: Branching ratio predictions for $\mu \rightarrow e + \gamma$ in the Albright - Barr model with $\tan \beta = 5$. In (a) A_0 is set equal to zero, while in (b) all three parameters, m_0 , $M_{1/2}$, A_0 , are allowed to vary.

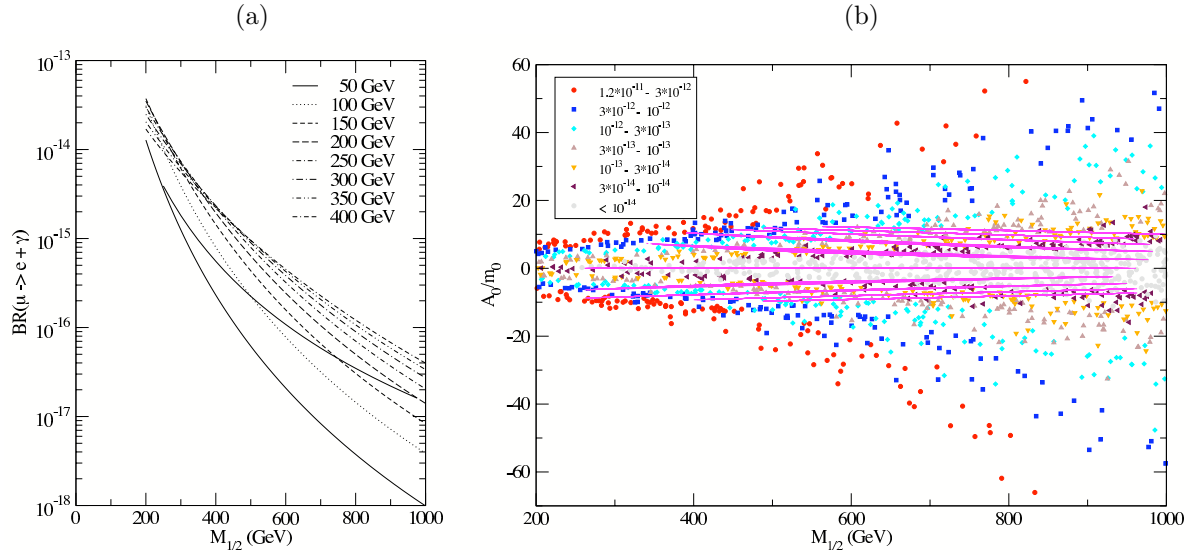


FIG. 4: Branching ratio predictions for $\mu \rightarrow e + \gamma$ in the Chen - Mahanthappa model with $\tan \beta = 10$.

For each model in Figs. 3(a), 4(a), 5(a), 6(a), and 7(a), we plot curves with constant values of m_0 indicated for the BR21 branching ratios as functions of $M_{1/2}$ with the trilinear coupling $A_0 = 0$ at the GUT scale. The curve which cuts across the m_0 curves in each left-hand plot represents the WMAP dark matter constraint for this value of A_0 . The horizontal broken line indicates the present experimental upper limit for this branching ratio [28].

In Figs. 3(b), 4(b), 5(b), 6(b), and 7(b), we allow A_0 to depart from zero and show scatterplots of A_0/m_0 vs. $M_{1/2}$. The points are color-coded as indicated according to the branching ratio intervals in which they fall, with all points below the present upper limit on the $\mu \rightarrow e\gamma$ branching

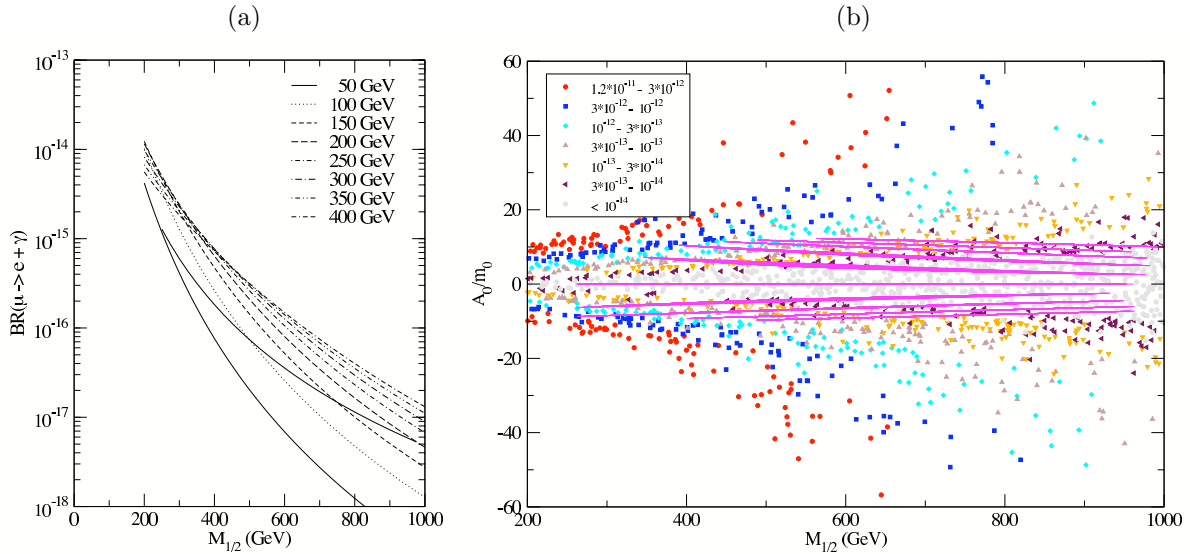


FIG. 5: Branching ratio predictions for $\mu \rightarrow e + \gamma$ in the Cai - Yu model with $\tan \beta = 10$.

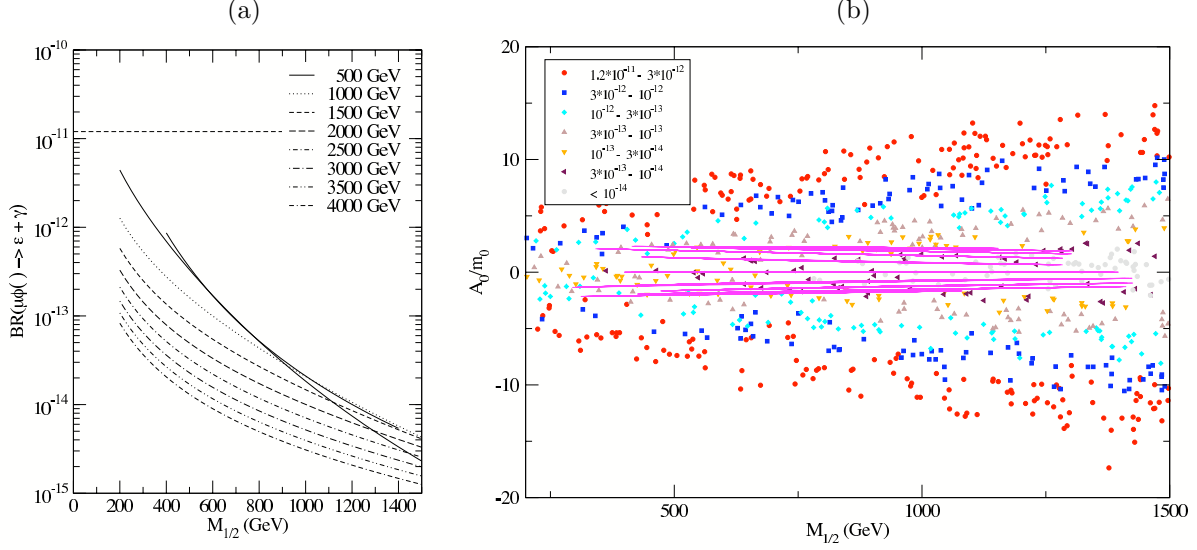


FIG. 6: Branching ratio predictions for $\mu \rightarrow e + \gamma$ in the Dermisek - Raby model with $\tan \beta = 50$.

ratio. The soft parameter constraints in Eq. (33) have been imposed for the Monte Carlo selection of points. The continuous curves represent the WMAP dark matter constraints and are drawn in steps of 500 GeV from $A_0 = -2.5$ TeV to $A_0 = 2.5$ TeV.

It is clear that the predicted branching ratio decreases as the universal soft gaugino mass at the GUT scale increases along the constant scalar mass curve. The Grimus-Kuhbock (GK) and Albright-Barr (AB) models will be probed first and then the Dermisek-Raby (DR) model by the MEG experiment, while the other two models are essentially beyond reach, if $A_0 = 0$ as depicted.

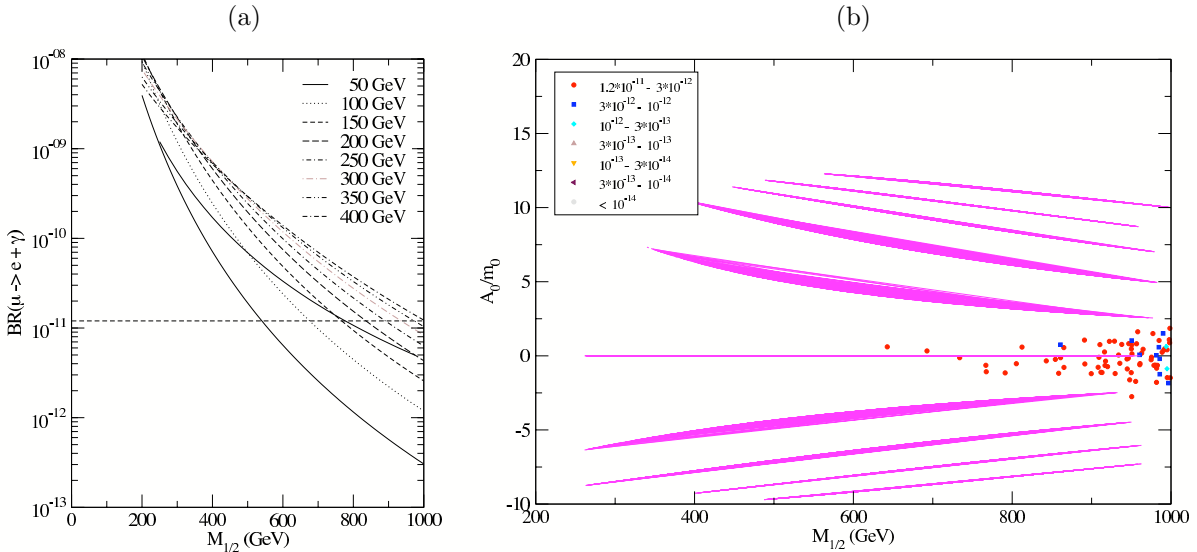


FIG. 7: Branching ratio predictions for $\mu \rightarrow e + \gamma$ in the Grimus - Kübock model with $\tan \beta = 10$.

One sees that higher values of BR21 are predicted for a given value of $M_{1/2}$ as $|A_0/m_0|$ increases. For the AB and GK models the experimental branching ratio greatly limits the allowed ranges of A_0/m_0 , while for the Chen-Mahanthappa (CM), Cai-Yu (CY), and DR models the dark matter constraints limit the allowed ranges of A_0/m_0 . In any case, the minimum predicted BR21 branching ratio occurs for $A_0 = 0$.

One can also present similar scatter plots for the $\tau \rightarrow \mu\gamma$ and $\tau \rightarrow e\gamma$ decay modes. Since all three decay modes are intimately related in each model through the corresponding logarithmic terms such as that in Eq. (32), the same scatter points will appear with only the color-coding changed (assuming one imposes the BR21 experimental limit for each plot).

Instead, we present two log-log plots for the BR32 and BR31 branching ratios against that for BR21 in Figs. 8 and 9, where $A_0 = 0$ has again been imposed. The thin line segments for each model observe the soft parameters constraints imposed, while the heavier line segments observe the more restrictive WMAP dark matter constraints. The vertical dashed line reflects the present BR21 bound, while the horizontal dashed line refers to the present BR32 or BR31 experimental

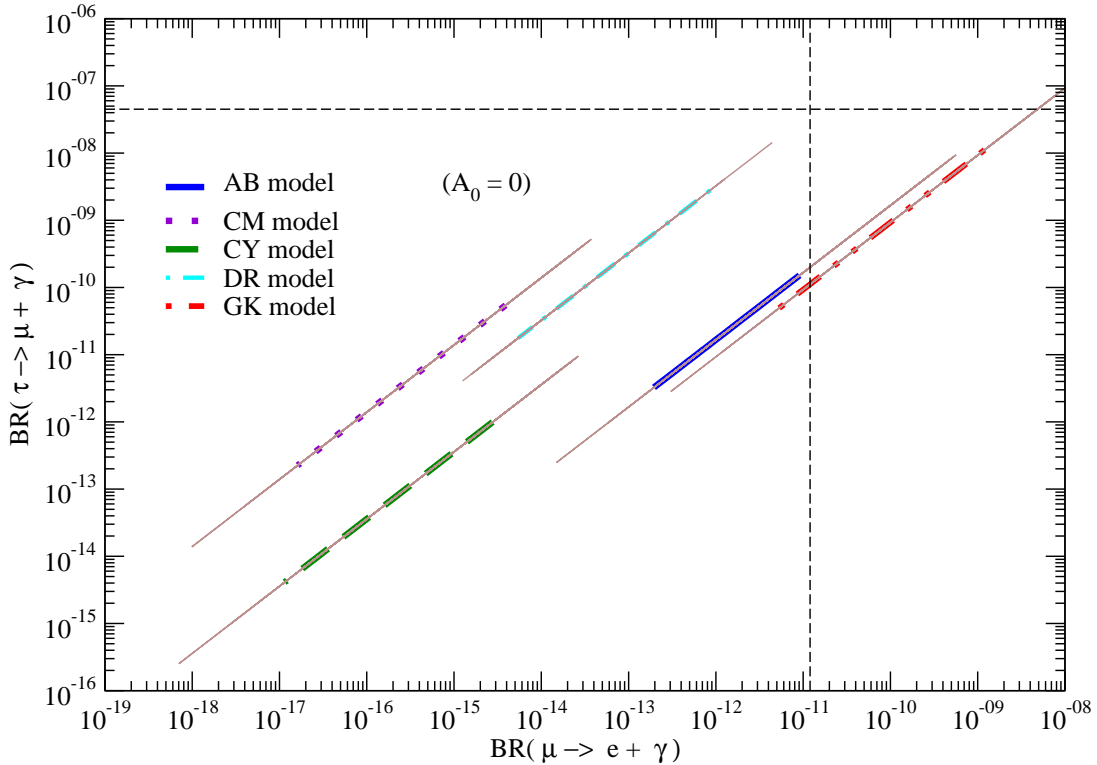


FIG. 8: Branching ratio predictions for $\tau \rightarrow \mu + \gamma$ vs. branching ratio predictions for $\mu \rightarrow e + \gamma$ in the five models considered. The soft-SUSY breaking constraints imposed apply for the thin line segments, while the more restrictive WMAP dark matter constraints apply for the thick line segments. The present experimental constraints are indicated by the dashed lines.

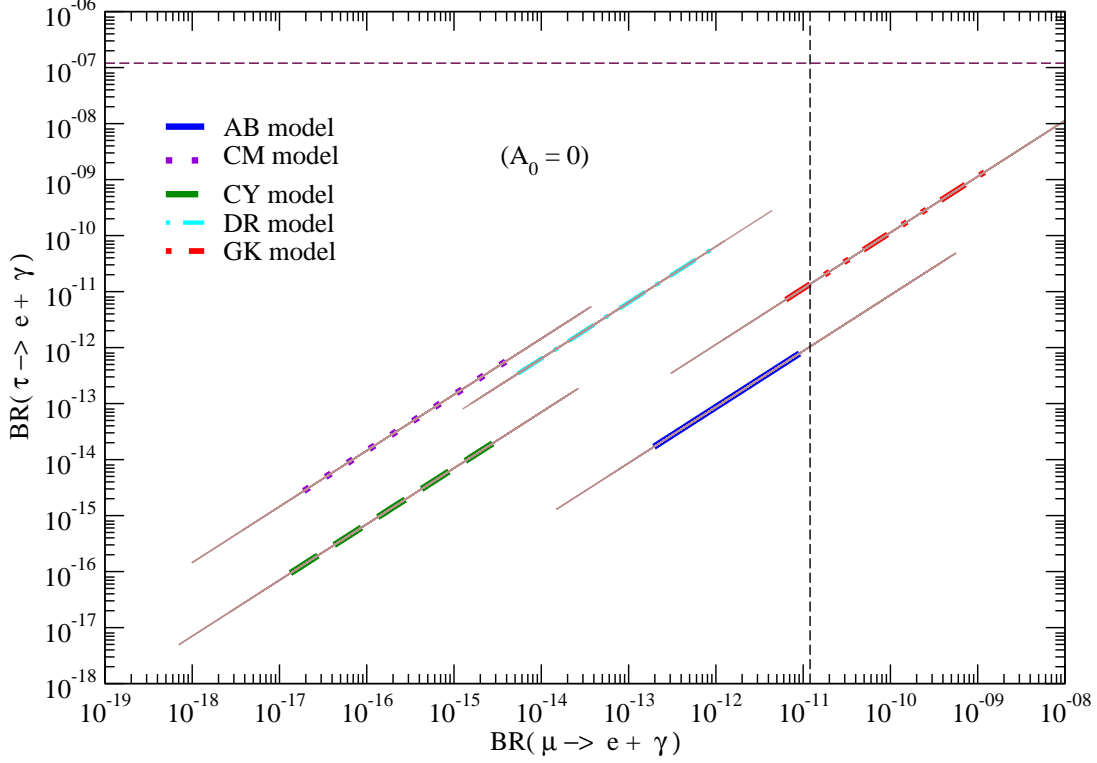


FIG. 9: Branching ratio predictions for $\tau \rightarrow e + \gamma$ vs. branching ratio predictions for $\mu \rightarrow e + \gamma$ in the five models considered. The soft SUSY breaking constraints imposed apply for the thin line segments, while the more restrictive WMAP dark matter constraints apply for the thick line segments.

limit, respectively [35]. It is clear from these two plots that the ongoing MEG experiment stands the best chance of confirming the predictions for or eliminating the GK and AB models. Even with a super-B factory [36], the present experimental bounds on the BR32 and BR31 branching ratios can only be lowered by one or two orders of magnitude at most.

But recall that the line segments apply for the special case of $A_0 = 0$. If one allows A_0 to depart

TABLE II: Ratios of the branching ratios for the lepton flavor violating τ decays and $\mu - e$ conversion on Ti relative to that for μ decay.

Models	$\text{BR}(\tau \rightarrow \mu\gamma)/\text{BR}(\mu \rightarrow e\gamma)$	$\text{BR}(\tau \rightarrow e\gamma)/\text{BR}(\mu \rightarrow e\gamma)$	$\text{BR}(\mu + Ti \rightarrow e + Ti)/\text{BR}(\mu \rightarrow e\gamma)$
AB	16.7	0.09	0.33
CM	1.3×10^4	171	0.11
CY	400	6.5	0.11
DR	3.3×10^3	61.0	0.026
GK	10.0	1.0	0.12

from zero, the line segments will slide diagonally upward and toward the right along their presently depicted positions by amounts that can be estimated from Figs. 3 - 7. Hence only the lower limits on the branching ratios are robust in Figs. 8, 9 and 11. However, it is clear that ratios of the branching ratios remain fixed for each model for any allowed A_0/m_0 . We present these ratios for the τ and $\mu - e$ conversion branching ratios relative to the $\mu \rightarrow e\gamma$ branching ratio in Table II. The spread in numbers for the ratios in different models appears to be greater than that anticipated by the authors of Ref. [37] for the class of models considered here.

In Table III we summarize the relevant findings from our study of the five models. The branching ratio ranges apply for the $A_0 = 0$ case and with the stricter WMAP dark matter constraints

TABLE III: Summary of the relevant results for the five $SO(10)$ SUSY GUT models considered in this work. The present experimental upper limits for the branching ratios are indicated in the second line, while the third line of the table gives the projected upper limit reaches for the Meg experiment, Super-B factory, and next generation $\mu - e$ conversion experiment.

Models	$\sin^2 \theta_{13}$	M_R 's (GeV)	$\tan \beta$	$ A_0/m_0 _{\max}$	BR21($\mu \rightarrow e\gamma$) $< 1.2 \times 10^{-11}$ $\rightarrow < 10^{-13}$	BR32($\tau \rightarrow \mu\gamma$) $< 4.5 \times 10^{-8}$ $\rightarrow < 10^{-9}$	BR($\mu + Ti \rightarrow e + Ti$) $< 4 \times 10^{-12}$ $\rightarrow < 10^{-18}$
AB	0.0020 (2.6°)	2.4×10^{14} 4.5×10^8 4.5×10^8	5	5	$(0.2 - 9) \times 10^{-12}$	$(0.03 - 1) \times 10^{-10}$	$(0.03 - 2) \times 10^{-12}$
CM	0.013 (6.5°)	7.0×10^{12} 4.5×10^9 1.1×10^7	10	12	$(0.02 - 4) \times 10^{-15}$	$(0.02 - 5) \times 10^{-11}$	$(0.01 - 3) \times 10^{-16}$
CY	0.0029 (3.1°)	2.4×10^{12} 2.4×10^{12} 2.4×10^{12}	10	12	$(0.02 - 5) \times 10^{-15}$	$(0.04 - 9) \times 10^{-13}$	$(0.03 - 6) \times 10^{-16}$
DR	0.0024 (2.8°)	5.8×10^{13} 9.3×10^{11} 1.1×10^{10}	50	2.5	$(0.05 - 8) \times 10^{-13}$	$(0.02 - 3) \times 10^{-9}$	$(0.01 - 2) \times 10^{-14}$
GK	0.00059 (1.4°)	2.1×10^{15} 4.2×10^{14} 6.7×10^{12}	10	2	$(0.4 - 80) \times 10^{-11}$	$(0.004 - 1) \times 10^{-8}$	$(0.02 - 5) \times 10^{-11}$

imposed. It is clear that the five predictive $SO(10)$ SUSY GUT models considered have very representative right-handed neutrino mass spectra and predictions for $\sin^2 \theta_{13}$. The CM, DR, and GK models have massive hierarchical spectra with M_3 ranging from 10^{13} to 10^{15} GeV. The CY model, on the other hand, has a degenerate spectrum with $M_R \sim 3 \times 10^{12}$ GeV, while the AB model has degenerate M_1 and M_2 which can lead to resonant leptogenesis. The CM model has a relatively large $\sin^2 \theta_{13}$ prediction which should be observable at the upcoming reactor neutrino experiments, Double CHOOZ and Daya Bay. The AB, CY and DR models have similar predictions for $\sin^2 \theta_{13}$ which will make observation of $\bar{\nu}_e \rightarrow \bar{\nu}_\mu$ oscillation somewhat marginal at those reactors and in the proposed NO ν A and T2K long-baseline experiments [38] without a SuperBeam source. For the GK model, the observation of such a low $\sin^2 \theta_{13}$ prediction would only take place with a Neutrino Factory. But it is clear from Table III and the previous figures that the GK and AB models will be tested first with the MEG experiment. From our discussion it is then clear that the LFV branching ratios are more sensitive to large M_3 than to large θ_{13} in the models considered. In previous generic studies of SUSY GUT models, the rare branching ratios were nearly equally sensitive to each of the two parameters [39].

IV. LEPTON FLAVOR VIOLATION IN $\mu - e$ CONVERSION

It is also of interest to consider lepton flavor violation in the μ to e conversion process in Titanium, $\mu + Ti \rightarrow e + Ti$. While there is no such ongoing experiment, preliminary discussion is underway to propose one which will lower the present limit. We shall see that the conversion rate predictions relative to the muon capture process, $\mu + Ti \rightarrow \nu_\mu + Sc$, are such that all five models considered in this paper can potentially be eliminated, if no signal is observed.

While predictions for the conversion process in the SM are infinitesimally small, large enhancements in the CMSSM framework again occur by virtue of massive super partners appearing in loop diagrams involving γ , Z and Higgs penguins and boxes. Of these, Arganda, Herrero and Teixeira have shown that the γ penguin contributions dominate the others by at least two orders of magnitude [40]. The slepton-neutralino and sneutrino-chargino loop contributions to the γ penguins are shown in Fig. 10. The virtual massive N^c and \tilde{N}^c with their Yukawa couplings again appear in the slepton loops along with a higgsino or Higgs particle, respectively.

The complex formulas for lepton flavor violation in this process were first derived by Hisano, Moroi, Tobe, and Yamaguchi [30]. If we restrict our attention to the γ penguin contribution as

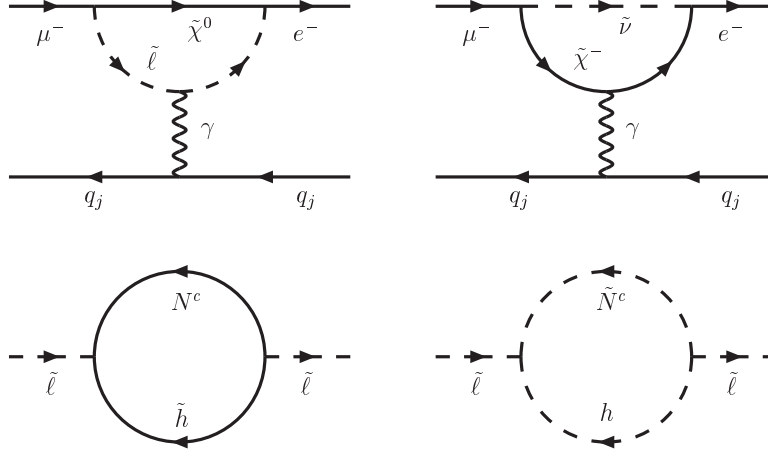


FIG. 10: Examples of Feynman diagrams for slepton - neutralino and sneutrino - chargino contributions to $\mu - e$ conversion in SUSY models with slepton mass insertions.

suggested by Arganda et al. [40], one finds the $\mu - e$ conversion rate is given by

$$\Gamma(\mu \rightarrow e) = 4\alpha^5 Z_{\text{eff}}^4 Z m_\mu^5 |F(q)|^2 [|A_1^L - A_2^R|^2 + |A_1^R - A_2^L|^2], \quad (35)$$

where here $A_1^{L,R}$ are form factors for the vertices connecting leptons of equal chirality, while $A_2^{L,R}$ are combinations of the electric dipole and magnetic dipole transition form factors previously denoted by $A_{L,R}$. For a ^{48}Ti target, $Z_{\text{eff}} = 17.6$ and the nuclear form factor is $F(q^2 \simeq -m_\mu^2) \simeq 0.54$ [30]. In the case of the conversion process, we have explicitly carried out the full evolution running from the GUT scale to the Z scale. The $\mu - e$ conversion branching ratio is then obtained from the conversion rate above by scaling it with the μ capture rate on Ti , which is quoted in [41] as $(2.590 \pm 0.012) \times 10^6 \text{ sec}^{-1}$ with the present experimental limit on the conversion branching ratio found to be $R \leq 4 \times 10^{-12}$.

In Fig. 11. we show a plot of the $\mu - e$ conversion branching ratio *vs.* the $\mu \rightarrow e\gamma$ branching ratio for each of the five models considered. We have limited the line segments by applying the WMAP dark matter constraints of Sec. III. It is clear that the GK and AB models would be tested first, followed by the DR, CY and CM models. In fact, a first generation $\mu - e$ conversion experiment may be able to reach a branching ratio of 10^{-17} , while a second generation experiment may lower the limit from the present value down to 10^{-18} [42]. If such proves to be the case and no signal is seen, all five models will be eliminated. Hence the conversion experiment is inherently more powerful than the MEG experiment looking for $\mu \rightarrow e\gamma$ which is designed to reach a level of $10^{-13} - 10^{-14}$, sufficient only to eliminate the GK and AB models. The caveat, of course, is that MEG is now starting to take data, while no new conversion experiment has been approved to date.

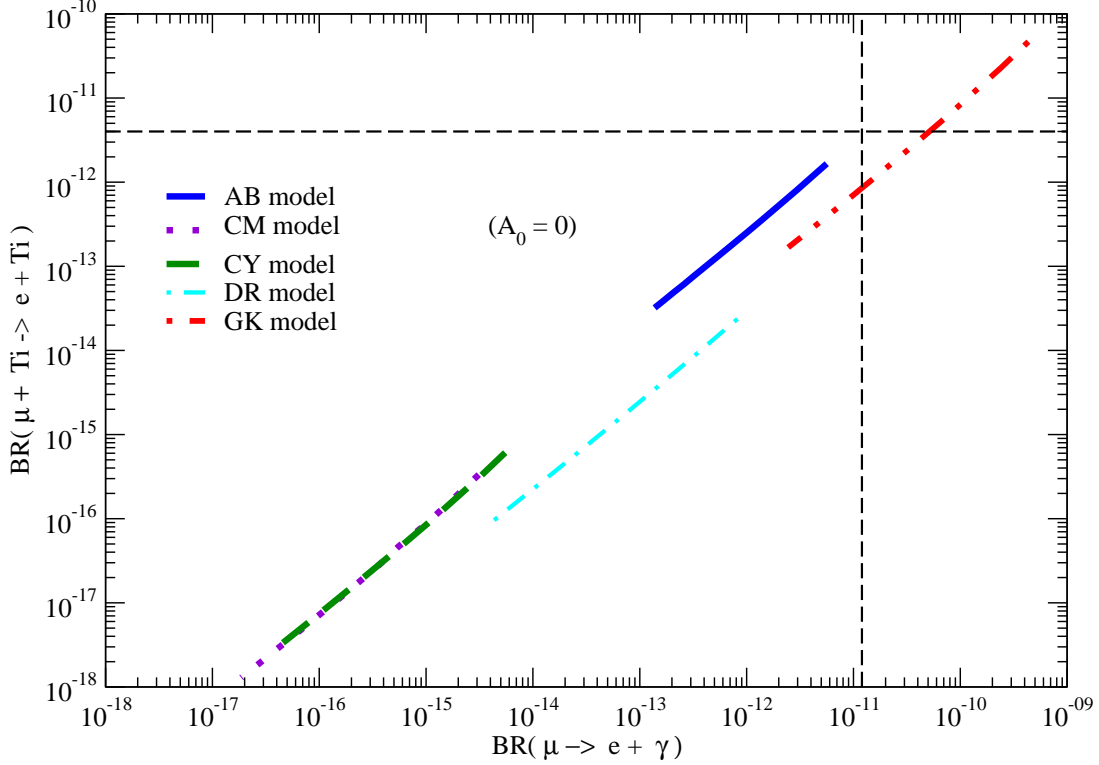


FIG. 11: Branching ratio predictions for $\mu - e$ conversion *vs.* branching ratio predictions for $\mu \rightarrow e + \gamma$ in the five models considered. Only thick line segments are shown reflecting the application of the more restrictive WMAP dark matter constraints. Note that the predictions for the CM and CY models overlap.

V. CONCLUSIONS

There have been many theoretical models constructed which aim to explain the neutrino masses and mixing patterns. While the predictions for the value of θ_{13} in these models may provide a way to distinguish some of these models, as shown in the survey over 63 models we have carried out in Ref. [5], the rare LFV processes, such as $\mu \rightarrow e + \gamma$ and $\mu - e$ conversion can provide an even more sensitive way to disentangle these models. We have investigated these rare processes in five SUSY SO(10) models that are currently still viable and highly predictive, making use of the allowed parameter space for the soft SUSY breaking parameters in the CMSSM framework. Utilizing the WMAP dark matter constraints, lower bounds on the branching ratios of these rare processes can be placed, and we find that at least three of the five models considered give rise to prediction for $\mu \rightarrow e + \gamma$ that will be tested at MEG. More interestingly, the next generation $\mu - e$ conversion experiment should be sensitive to the predictions of all five models, making it an even more robust way to test these models. While generic studies have emphasized the important dependence of the branching ratios on the reactor neutrino angle, θ_{13} , and the mass of the heaviest

right-handed neutrino, we find the latter to be by far the more significant in the models tested.

ACKNOWLEDGMENTS

We thank Stephen Martin for making available to us his evolution program for the Yukawa couplings and soft SUSY breaking parameters. The work of M.-C.C. is supported, in part, by the National Science Foundation under Grant No. PHY-0709742. One of us (C.H.A.) thanks the members of the Theory Group at Fermilab for their kind hospitality. Fermilab is operated by the Fermi Research Alliance under contract No. DE-AC02-07CH11359 with the U.S. Department of Energy.

Note added.—After completion of this work, the authors of Ref. [43] informed us that a suppression factor should be applied to the lepton flavor violating branching ratios calculated in our paper. This suppression arises from a QED radiative correction to the effective dipole operators responsible for the rare decays. The multiplicative factor in question is given by $1-\delta$, where $\delta = (8\alpha/\pi) \log(\Lambda/m_j)$, $\Lambda \sim 250 - 1000$ GeV is the sparticle mass scale responsible for the LFV, and $m_j = m_\mu$ or m_τ for the rare radiative muon or tau decays. For $\mu \rightarrow e\gamma$, the δ correction amounts to roughly 0.15, so the branching ratio is about 0.85 times the rate given in the paper. The authors thank Andrzej Czarnecki and Ernest Jankowski for pointing out their earlier work to them.

-
- [1] Y. Ashie *et al.* (Super-Kamiokande Collaboration), Phys. Rev. D **71**, 112005 (2005); J. Hosaka *et al.* (Super-Kamiokande Collaboration), Phys. Rev. D **73**, 112001 (2006); B. Aharmim *et al.* (SNO Collaboration), Phys.Rev. C **72**, 055502 (2005);
 - [2] M. Apollonio *et al.* (CHOOZ Collaboration), Phys. Lett.B **420**, 397 (1998); *ibid.*, Eur. Phys. J C **27**, 331 (2003); F. Boehm *et al.* (Palo Verde Collaboration), Phys.Rev. D **64**, 112001(2001); T. Araki *et al.* (KamLAND Collaboration), Phys.Rev.Lett.**94**, 081801 (2005); S. Abe *et al.* (KamLAND Collaboration), arXiv:0801.4589.
 - [3] M. Ahn *et al.* (K2K Collaboration), Phys. Rev. D **74**, 072003 (2006); D.G. Michael *et al.* (MINOS Collaboration), Phys. Rev. Lett. **97**, 191801 (2006); (MINOS Collaboration), arXiv:0708.1495.
 - [4] M. Maltoni, T. Schwetz, M.A. Tortola and J.W.F. Valle, New J. Phys. **6**, 122 (2004).
 - [5] C.H. Albright and M.-C. Chen, Phys. Rev. D **74**, 113006 (2006).
 - [6] F. Borzumati and A. Masiero, Phys. Rev. Lett. **57**, 961 (1986).
 - [7] For recent reviews, see, e.g. M.-C. Chen and K. T. Mahanthappa, Int. J. Mod. Phys. A **18**, 5819 (2003); AIP Conf. Proc. **721**, 269 (2004); G. Altarelli and F. Feruglio, New J. Phys. **6**, 106 (2004); S.F. King, Rept. Prog. Phys. **67**, 107 (2004); Z.z. Xing, Int. J. Mod. Phys. A **19**, 1 (2004); R.N.Mohapatra, New

- J. Phys. **6**, 82 (2004); A. Yu. Smirnov, Int. J. Mod. Phys. A **19** 1180 (2004); R.N. Mohapatra and A.Y. Smirnov, Ann. Rev. of Nucl. and Part. Sci., **56**, 569 (2006); R.N. Mohapatra *et al.*, Rep. Prog. Phys. **70**, 1757 (2007); A. Strumia and F. Vissani, arXiv:hep-ph/0606054.
- [8] A. Masiero, S.K. Vempati, and O. Vives, Nucl. Phys. **B649**, 189 (2003); New J. Phys. **6**, 202 (2004); F. Deppisch, H. Päs, A. Redelbach, R. Rückl, and Y. Shimizu, Eur. Phys. J. C **28**, 365 (2003); F. Deppisch, H. Päs, R. Rückl, and A. Redelbach, Phys. Rev.D **73**, 033004 (2006); E. Arganda and M.J. Herrero, Phys. Rev. D **73**, 055003 (2006); L. Calibbi, A. Faccia, A. Masiero, and S.K. Vempati, J. High Energy Phys. **7**, 012 (2007).
- [9] J.A. Casas and A. Ibarra, Nucl. Phys. **B618**, 171 (2001).
- [10] A. Kageyama, S. Kaneko, N. Shimoyama, and M. Tanimoto, Phys. Lett. B **527**, 206 (2002); Q. Shafi and Z. Tavartkiladze, Nucl. Phys. **B772**, 133 (2007); **B778**, 216(E) (2007); S. Antusch and S.F. King, Phys. Lett. B **659**, 640 (2008). An earlier test of one of the models considered in this work for the $\mu \rightarrow e\gamma$ branching ratio was published in E. Jankowski and D.W. Maybury, Phys. Rev. D **70**, 035004 (2004).
- [11] P. Minkowski, Phys. Lett. B **67**, 421 (1977); T. Yanagida, in *Proceedings of the Workshop on the Unified Theory and Baryon Number in the Universe, Tsukuba, Japan 1979*, edited by O. Sawada and A. Sugamoto (KEK, Tsukuba, 1979), p. 95; M. Gell-Mann, P. Ramond, and R. Slansky, in *Supergravity*, edited by P. van Nieuwenhuizen and D. Z. Fredman (North-Holland, Amsterdam, 1979), p. 315; S.L. Glashow, in *Proceedings of the 1979 Cargese Summer Institute on Quarks and Leptons*, edited by M. Levy, J.-L. Basdevant, D. Speiser, J. Weyers, R. Gastmans, and M. Jacob (Plenum Press, New York, 1980), p. 687; R.N. Mohapatra and G. Senjanovic, Phys. Rev. Lett. **44**, 912 (1980).
- [12] B. Pontecorvo, Zh. Eksp. Teor. Fiz. **33**, 549 (1957) [Sov. Phys. JETP **6**, 429 (1957)]; Z. Maki, M. Nakagawa and S. Sakata, Prog. Theor. Phys. **28**, 870 (1962).
- [13] Review of Particle Physics, W.-M. Yao et al., J. Phys. G **33**, 1 (2006).
- [14] K.S. Babu and R.N. Mohapatra, Phys. Rev. Lett. **70**, 2845 (1993).
- [15] K.S. Babu and S.M. Barr, Phys. Lett. B **381**, 202 (1996); C.H. Albright, K.S. Babu, and S.M. Barr, Phys. Rev. Lett. **81**, 1167 (1998).
- [16] C.H. Albright, Phys. Lett. B **599**, 285 (2004).
- [17] C.H. Albright and S.M. Barr, Phys.Rev. D **64**, 073010 (2001).
- [18] C.H. Albright, Phys. Rev. D **72**, 013001 (2005); **74**, 039903(E) (2006).
- [19] A. Pilaftsis and T.E.J. Underwood, Nucl. Phys. **B692**, 303 (2004).
- [20] M.-C. Chen and K.T. Mahanthappa, Phys. Rev. D **70**, 113013 (2004).
- [21] Y. Cai and H.-B. Yu, Phys. Rev. D **74**, 115005 (2006).
- [22] R. Dermisek and S. Raby, Phys.Lett. B **622**, 327 (2005).
- [23] W. Grimus and H. Kühbock, Phys. Lett. B **643**, 182 (2006).
- [24] S.A. Dazley (Double CHOOZ Collaboration), in Proceedings of NuFACT05, Nucl. Phys. B, Proc. Suppl. **155**, 231 (2006); J. Cao (Daya Bay Collaboration), *ibid.* **155**, 229 (2006).

- [25] M. Apollonio *et al.* (CHOOZ Collaboration), Phys. Lett. B **420**, 397 (1998); Eur. Phys. J. C **27**, 331 (2003); cf. also F. Boehm *et al.* (Palo Verde Collaboration), Phys.Rev. D **64**, 112001(2001).
- [26] B.W. Lee and R.E. Shrock, Phys. Rev. D **16**, 1444 (1977).
- [27] A. Baldini, Nucl. Phys. B, Proc. Suppl. **168**, 334 (2007).
- [28] M.L. Brooks *et al.* (MEGA Collaboration), Phys. Rev. Lett. **83**, 1521 (1999).
- [29] For references to the CMSSM, cf. K.A. Olive, submitted to the SUSY07 proceedings arXiv:0709.3303.
- [30] J. Hisano, T. Moroi, K. Tobe, and M. Yamaguchi, Phys. Rev. **53**, 2442 (1996).
- [31] S.T. Petcov, S. Profumo, Y. Takanishi, and C.E. Yaguna, Nucl. Phys. **B676**, 453 (2004).
- [32] D.N. Spergel *et al.* (WMAP Collaboration), Astrophys. J. Suppl. Ser. **170**, 377 (2007).
- [33] P. Binetruy, G. Girardi, and P. Salati, Nucl. Phys. **B237**, 285 (1984); K. Griest and D. Seckel, Phys. Rev. D **43**, 3191 (1991).
- [34] L.S. Stark, P. Häfliger, A. Biland, and F. Pauss, J. High Energy Phys. **0508**, 059 (2005).
- [35] B. Aubert *et al.* (BABAR Collaboration), Phys. Rev. Lett. **96**, 041801 (2006); **95**, 041802 (2005); K. Abe *et al.* (Belle Collaboration), in *Proceedings of the ICHEP06 Conference, Moscow, 2006*.
- [36] A.G. Akeroyd *et al.* (SuperKEKB Physics Working Group), arXiv:hep-ex/0406071.
- [37] V. Cirigliano, A. Kurylov, M.J. Ramsey-Musolf, and P. Vogel, Phys. Rev. Lett. **93**, 231802 (2004).
- [38] Y. Hayato *et al.* (T2K Collaboration), Nucl. Phys. B, Proc. Suppl. **143**, 269 (2005); D.S. Ayres *et al.*, Technical Design Report for the NO ν A Experiment E929 at Fermilab, 2007.
- [39] S. Antusch, E. Arganda, M.J. Herrero, and A.M. Teixeira, J. High Energy Phys. **11**, 090 (2006), cf. Ref. [8].
- [40] E. Arganda, M.J. Herrero, and A.M. Teixeira, J. High Energy Phys. **10**, 104 (2007).
- [41] C. Dohmen *et al.* (SINDRUM II Collaboration), Phys. Lett. B **317**, 631 (1993).
- [42] W. Molzon, in *Fermilab Program Planning Report Presented before the P5 Committee, January 2008*.
- [43] A. Czarnecki and E. Jankowski, Phys. Rev. D **65**, 113004 (2002).